Available online at www.sciencedirect.com
ScienceDirect
Journal of Catalysis 248 (2007) 20–28
JOURNAL OF CATALYSIS
www.elsevier.com/locate/jcat

Understanding the enhancement of catalytic performance for olefin cracking: Hydrothermally stable acids in P/HZSM-5

Nianhua Xue [a], Xiangke Chen [a], Lei Nie [a], Xuefeng Guo [a], Weiping Ding [a,*], Yi Chen [a], Min Gu [b], Zaiku Xie [c]

[a] *Laboratory of Mesoscopic Chemistry, School of Chemistry and Chemical Engineering, Nanjing University, Nanjing 210093, PR China*
[b] *Department of Physics, Nanjing University, Nanjing 210093, PR China*
[c] *Shanghai Research Institute of Petrochemical Technology, Shanghai 201208, PR China*

Received 4 December 2006; revised 13 February 2007; accepted 21 February 2007

Abstract

Enhanced catalytic performance for C_4 olefin cracking to propene and ethene was observed on phosphorus-modified HZSM-5 treated in steam at 1073 K. Combining the results of ^{31}P and ^{27}Al MAS NMR, D_2/OH exchange, NH_3-TPD, and catalytic performance of the catalysts, it seems reasonable to conclude that new and hydrothermally stable acid sites are formed during the steam treatment through the interaction of phosphorus species with silanol nests exposed on the zeolite due to dealumination. It is tentatively suggested that the incorporated phosphorous species stabilized by some nonframework aluminum species are responsible for both the enhanced acid stability and the significantly improved catalytic performance for the cracking of C_4 olefin.

Keywords: P/HZSM-5; Hydrothermal stability; D_2/OH exchange; Olefin cracking

1. Introduction

Coke formation in the hydrocarbon reactions over acidic zeolite catalysts inhibits their activity for further reaction by covering their surface acid sites and/or blocking the access path of the reactants [1]. Adding an appropriate amount of steam in the feedstock is a well-known method to prevent or reduce coke formation [2]; in fact, hydrothermally stable solid acids have been necessary to a series of catalytic processes and attracted much research attention in the past decades. Due to the rapidly growing demand for propene, the catalytic cracking of low-value C_4 olefins to propene has drawn much interest [3–8]. HZSM-5 is an effective catalyst for this reaction; but overcoming its instability at high temperature in steam caused by dealumination is crucial for its practical application. Phosphorus-modified HZSM-5 has shown noticeably improved hydrothermal stability [9–13]; adding P has a positive effect on the acidity of the catalyst, especially its Brönsted acidity, as indicated by TPD and IR spectroscopic characterizations [14–20]. The states of aluminum and phosphorus in the phosphorus-modified HZSM-5 have been identified by MAS NMR [9,11,21–28]. Several models relating to the structure of the HZSM-5 acid sites modified by phosphorus have been proposed, as summarized by Corma et al. [13]. Védrine et al. [14] and Kaeding et al. [15] have suggested that phosphorus species are bonded to the zeolite framework through oxygen in the form of elemental phosphorus of 5^+ oxidation state. Lercher et al. [16] have proposed that the phosphorus species were interacted with the oxygen of the bridging hydroxyl groups by replacing the protons on them and resulting in the broken of the Al–O bonding and the opening of the zeolite framework. According to the model of Corma et al., the incorporated phosphorus species were in the form of tetrahydroxyphosphonium cations $P(OH)_4^+$ on ZSM-5 [13]. Recently, Cerqueira et al. proposed another distorted tetrahedral Al to be active in n-hexane cracking besides framework Al in H-MFI zeolites [27].

---

[*] Corresponding author. Fax: +86 25 83686251.
E-mail address: dingwp@nju.edu.cn (W. Ding).

0021-9517/$ – see front matter © 2007 Elsevier Inc. All rights reserved.
doi:10.1016/j.jcat.2007.02.022

Table 1
Phosphorus content in P/HZSM-5 determined by XRF

Samples	P content[a] (wt%)	P lost (%)[b]
0.9P-Z	0.72 (232)	–
1.8P-Z	1.68 (542)	–
2.7P-Z	2.20 (710)	–
0.9P-ZH4	0.68 (219)	4.6
1.8P-ZH4	1.54 (496)	8.3
2.7P-ZH4	1.85 (597)	15.9

[a] The figures in parenthesis are the number of P atoms (μmol g^{-1}).
[b] The P lost during the steam treatment at 1073 K.

Most related studies have taken the viewpoint that the hydrothermally stable acid sites of the modified HZSM-5 originate from the framework aluminum being protected from dealumination. The changes in the structure of the modified acid sites during hydrothermal treatment have scarcely been investigated, and few convincing results on the phosphorous status under hydrothermal conditions in the modified HZSM-5 have been elucidated to date. It seems that the details of the interaction between P and HZSM-5 and the nature of the acid sites thus induced are worthy of further clarification, because they are closely related to the anticoke deposition as well as the catalytic behavior of the catalyst. We herein demonstrate the influences of hydrothermal treatment on the Brönsted acid sites of the HZSM-5 modified by phosphorus using various experimental techniques, including D_2/OH-exchange measurements, temperature-programmed desorption of ammonia, ^{31}P MAS NMR, and others. The effects of phosphorus modification and steam treatment on the catalytic performance of these catalysts for C_4 olefin cracking also are reported.

2. Experimental

2.1. Materials

HZSM-5 (Si/Al = 35, Shanghai Research Institute of Petrochemical Technology) was impregnated with $(NH_4)_2HPO_4$ solution under stirring, and the slurry was evaporated at 353 K and dried overnight at 393 K. The resulted powders were then heated in flowing air (60 ml min^{-1}) to 843 K at a rate of 2 K min^{-1} and calcined at that temperature for 6 h. Then the samples were pressed and crushed to particles of 20–40 mesh for catalytic testing and characterization. The phosphorus contents were 0.7, 0.9, 1.4 (the amount of P in this particular sample is equal to the number of its framework aluminum), 1.8, and 2.7 wt%. These catalysts were designated 0.7P-Z, 0.9P-Z, 1.4P-Z, 1.8P-Z, and 2.7P-Z, respectively. The actual P contents were determined by X-ray fluorescence (XRF) and are listed in Table 1. Hydrothermal treatment was performed in a stainless steel reactor. The temperature was increased at a rate of 5 K min^{-1} to 1073 K, and liquid water ($\sim$0.1 g min^{-1}) was pumped into the preheated zone of the reactor. The steam then traveled through the sample bed. Any carrier gases were not used. The samples were hydrothermally treated at 1073 K for 4 h and designated 0.7P-ZH4, 0.9P-ZH4, 1.4P-ZH4, 1.8P-ZH4, and 2.7P-ZH4. Samples 0.9P-ZH12, 0.9P-ZH24, and 0.9P-ZH48 were 0.9P-Z treated in 100% steam at 1073 K for 12, 24, and 48 h, respectively.

Some special samples were designed to verify the hypothesis about the nature of the acid sites of HZSM-5 modified by P and hydrothermally treated at high temperature. First, the HZSM-5 (Al content, 463 μmol g^{-1}) was steamed in 100% steam at 1073 K for 4 h and washed with EDTA solution to remove weakly bonded aluminum caused by dealumination [29]; this sample was designated S-Z in this context, in which aluminum content was 224 μmol g^{-1} (XRF result). The S-Z was then treated in aqueous solution of $(NH_4)_2HPO_4$ at 443 K in a Teflon-lined autoclave for 55 h. The resulting sample was filtered and thoroughly washed to remove excessive phosphorus. This sample, designated HP-Z in this context, contained 224 μmol g^{-1} of aluminum and 101 μmol g^{-1} of phosphorus (XRF analysis). EHP-Z was synthesized at the same conditions with the HP-Z, but excessive phosphorus was retained by evaporation during postsynthesis, in which the P content was 295 μmol g^{-1} (XRF). RHP-Z was synthesized at the same conditions with HP-Z by hydrothermal reaction of $(NH_4)_2HPO_4$ with fresh HZSM-5 at 443 K in a Teflon-lined autoclave; almost no P was detected in this sample by XRF.

2.2. Characterization

2.2.1. NH_3-TPD

Catalyst samples (100 mg) were cleaned in 80 ml min^{-1} He (ultra-high-purity grade) at 873 K for 1 h and then cooled to 423 K in helium. The adsorption of ammonia was performed at this temperature. After flushing by pure He, TPD of ammonia was performed at 10 K min^{-1} to 873 K. The signal was recorded by a thermal conductivity detector. The density of strong acid sites was defined and detected by NH_3-TPD with ammonia adsorption at 573 K.

2.2.2. D_2/OH exchange

First, the catalyst samples (400 mg) were activated in 100 ml min^{-1} 20% O_2/Ar (ultra-high-purity grade) at 10 K min^{-1} to 723 K, soaked at this temperature for 1 h, and then cooled in Ar (80 ml min^{-1}) to room temperature. Deuterium exchanged with protonium presented in the samples was measured by increasing the temperature to 1073 K at 10 K min^{-1}. The signal of HD molecules was monitored by mass spectrometry (Inficon Transpector 2). Ar was used as an internal standard to calculate the formation of HD during the exchange between D_2 and hydroxyls in the samples.

2.2.3. Porous texture

The specific surface areas and pore volumes of the catalysts were obtained by means of nitrogen adsorption measurements at 77 K using a Micrometrics ASAP 2020 instrument. Samples were treated at 623 K under vacuum before N_2 adsorption. Total surface area was calculated using the classical BET method, and pore volume was evaluated with the t-plot method using the equation of Harkins and Jura. The content of phosphorous was determined by X-ray fluorescence using an ARL-9800 spectrometer.

2.2.4. NMR measurements

^{31}P NMR spectra were measured on a Bruker AV-300 solid-state NMR spectrometer operating at a field of 7.0 T with a standard Bruker solid MAS probe. The zirconium dioxide rotors were spun at 8 kHz with dry air as the driving gas. The pulse widths were 2.2 µs ($\pi/2$), with a 15-s repetition time and 2000 scans. A chemical shift was reported with respect to H_3PO_4. ^{27}Al NMR spectra were recorded at 78.2 MHz with a spinning rate of 8 kHz and pulse widths of 0.5 µs with a 1-s repetition time. ^{27}Al chemical shifts were reported relative to $[Al^{3+}(H_2O)_6]$. The NMR analysis was carried out with the samples prehydrated in a wet desiccator for several days.

2.2.5. Crystal lattice parameters

XRD patterns of the samples were recorded in the 2θ region of 5°–40° using a diffractometer (Shimadzu XRD-6000) with Cu$K\alpha$ radiation ($\lambda = 1.5418$ Å). The scan speed was set at $1° \text{ min}^{-1}$ with a step size of 0.02°. Silicon powder was blended into the samples as an internal standard for calibration of 2θ. The crystal parameters were refined from six reflections on basis of orthorhombic system of HZSM-5.

2.2.6. Catalytic test

The butene cracking reaction was carried out in a continuous-flow, fixed-bed system. A 0.85-g catalyst sample was placed in a stainless steel tubular reactor (8 mm i.d.) and then heated to and maintained at 803 K for 2 h in flowing nitrogen. Then the nitrogen was switched to C_4 gases containing 84 vol% butene and 16 vol% butane and diluted in nitrogen ($N_2/C_4 = 3$) at LHSV of $10\ h^{-1}$. The total pressure of the reaction gas was 101 kPa. Reaction products were analyzed online by gas chromatography with a 50-m fused silica Chrompack PLOT Al_2O_3/Na_2SO_4 capillary column and a flame ionization detector.

3. Results and discussion

3.1. Solid-state NMR

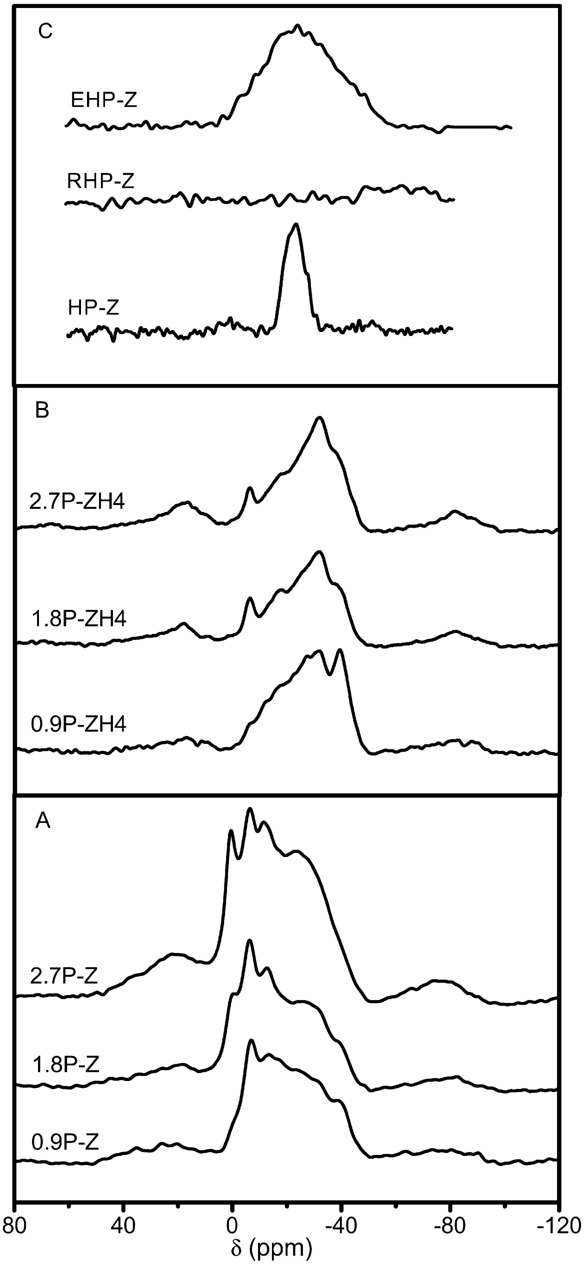

Fig. 1. ^{31}P MAS NMR spectra of P/HZSM-5. (A) before hydrothermal treatment; (B) after hydrothermal treatment; (C) HP-Z was synthesized with $(NH_4)_2HPO_4$ reacting with dealuminated (1073 K, 100% steam) and EDTA treated HZSM-5 at 443 K in Teflon lined autoclave for 55 h. RHP-Z was synthesized similar to HP-Z but with fresh HZSM-5. EHP-Z was synthesized similar to HP-Z but excessive $(NH_4)_2HPO_4$ in solution was retained by evaporating the solution to dry.

Fig. 1 shows the ^{31}P MAS NMR spectra of the P-containing samples. The spectra of phosphorus-impregnated HZSM-5 before (Fig. 1A) and after steam treatment at 1073 K (Fig. 1B) exhibited a broad response in a wide field due to the complicated environment of the phosphorus species in the samples. The peak at 0 ppm is associated with the excess phosphorus compound, which interacted very weakly with the zeolite [21]. The peak at −6 ppm is due to the terminal phosphorus atoms in pyrophosphoric acid species [9,21,25,26]. The resonance at −12 ppm represents the middle phosphorus atoms in polyphosphates or some specially polymerized short-chain polyphosphates [26]. The above assignments seem to be reliable and less controversial in the literature. A broad line at about −40 ppm is tentatively ascribed to phosphorus reacted with impurities or vacancies in the zeolite structure [21]. The phosphorus with a chemical shift at −46 ppm is known for branching groups in the compounds like P_4O_{10} [25,26]. It can be inferred from the signal at 0 ppm in ^{31}P MAS NMR spectra before hydrothermal treatment that the 1.8P-Z and 2.7P-Z samples contained much excessive phosphorus and interacted only weakly with the zeolite, even though they were calcined at 843 K in dry air.

After steam treatment (Fig. 1B), the broad resonances with maximum at −32 ppm were observed for all three samples related to extra-framework aluminum phosphate [9]. Some authors have tentatively assigned the remaining broad signals in the range of −20 to −30 ppm to highly condensed polyphosphate species and/or extra-framework aluminum phosphate [30,31], but this assignment seems controversial and not

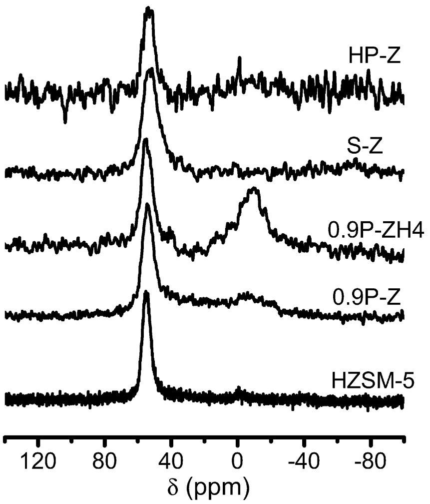

Fig. 2. ^{27}Al MAS NMR spectra of P/HZSM-5. The meanings of the samples are the same with those in Fig. 1.

so convincing. As we discuss below, some unique phosphorus species formed in hydrothermal process may be included in the broad response and may be difficult to distinguish due to serious overlap with other species.

HP-Z was synthesized to obtain single phosphorus species in HZSM-5. Its ^{31}P NMR spectrum shows relatively narrow signals centered at -23 ppm along with a shoulder peak at -28 ppm (Fig. 1C). These findings imply the formation of basically single phosphorus species during postsynthesis. Comparatively, no phosphorus species were found in the RHP-Z sample by NMR measurements and chemical analysis (not shown), indicating that phosphate could not react at 443 K in solution with fresh HZSM-5, with which dealumination treatment was not performed. This leads to conclusion that phosphates react readily with the vacancies formed by dealumination, giving rise to new phosphorus species in HZSM-5 with ^{31}P NMR resonance at about -23 ppm. The P species with a chemical shift at -23 ppm can be assigned to new P species, formed by the reaction of phosphate with the silanol nests left by dealumination. A special structure of the phosphorous species could be expected during steam treatment at 1073 K. When excessive phosphate (exceeding the number of vacancies formed in dealumination) was reserved, as in sample EHP-Z, a broad resonance response of ^{31}P NMR appeared, with even species similar to P_4O_{10} (~ -46 ppm) and silicon pyrophosphate (~ -54 ppm) detected (Fig. 1C) [32].

Fig. 2 shows the ^{27}Al MAS NMR spectra of the P/HZSM-5 samples. The spectrum of the HZSM-5 consists of the signal at 55 ppm of framework tetrahedral Al and the much weaker signal at 0 ppm related to typical extra-framework octahedral aluminum. A similar spectrum was obtained for the 0.9P-Z sample but with a weak signal of octahedral Al -14 ppm along with one at 0 ppm. A broad band became evident at ca. 36 ppm, which is usually attributed to tetrahedral aluminum in a distorted environment at either framework [33] or nonframework positions [34–36]. Phosphorus modification resulted in slight dealumination. When 0.9P-Z was steamed at 1073 K for 4 h, dealumination was detected despite the protection effect of phosphorus on framework alumina as proposed previously. The ^{27}Al spectrum of 0.9P-ZH4 shows the signal at 55 ppm with decreased intensity and the signals at 0 to -14 ppm with increased intensity, reflecting the dealumination occurring during steaming.

For the S-Z sample, almost no typical extra-framework octahedral aluminum at 0 ppm was detected, demonstrating that the extra-framework and octahedral aluminum was effectively removed by washing with the EDTA solution. Because the density of residual OH groups of S-Z was 126 μmol g^{-1} (detected by D_2/OH exchange and presented below), and the XRF results revealed 224 μmol g^{-1} of aluminum remaining in the zeolite, the excessive aluminum can likely be ascribed to invisible nonframework aluminum in the amount of $\sim$100 μmol g^{-1}. The invisible Al released from the framework formed not only Al ions, but also Al–O and Si–O–Al–O phases, which also may incorporate P additives.

For HP-Z, the response of framework aluminum shifted from $\sim$54.8 to 53.6 ppm of HZSM-5 with broadened width, indicative of the changed environment of framework aluminum led by phosphorus modification. This sample contained about 101 μmol g^{-1} of phosphorus combined with the zeolite during the hydrothermal reaction in solution. There also were weak signals in the region of 45 to -14 ppm ascribed to tetrahedral Al in a distorted environment, intermediate aluminum species, classical octahedral Al in extra-framework, and octahedral Al attached to phosphorous [27].

3.2. D_2/OH exchange

HD formation in D_2/OH exchange is a quantitative measurement of solid surface hydroxyls [37–40]. The amount of HD reflects the number of OH groups on the surface, and the temperature of exchange relates to the acid property to some extent, provided that the acid structure is similar. For the current samples, the D_2/OH exchange is driven basically by heat; these samples lacked sites for deutonium dissociation.

Fig. 3 displays the HD evolution with the increasing temperature of the samples. For the fresh HZSM-5, an HD evolution peak was observed at 760 K, mainly from zeolitic hydroxyls. The total number of the hydroxyls was 502 μmol g^{-1}, as shown in Fig. 3A. When modified with phosphorous, the peak temperatures for D_2/OH exchange were regularly postponed to 785, 802, 811, 835, and 847 K for 0.7P-Z, 0.9P-Z, 1.4P-Z, 1.8P-Z, and 2.7P-Z, respectively, reflecting the higher barriers for D_2/OH exchange with increased phosphorus doping. Moreover, the density of the OH groups decreased with increasing amounts of phosphorus, because the interaction of phosphate root with zeolitic OH groups eliminates the zeolitic OH groups, and the condensation between phosphate roots will decrease the number of OH groups. The decrease in OH groups was most significant for the 0.7P-Z sample.

Interestingly, big changes in the HD evolution profiles were observed after these samples were steam treated at 1073 K, reflecting changes in status or the environment of OH groups of P/HZSM-5 during treatment, as shown in Fig. 3B. The OH density of HZSM-5 was reduced significantly after treatment, with

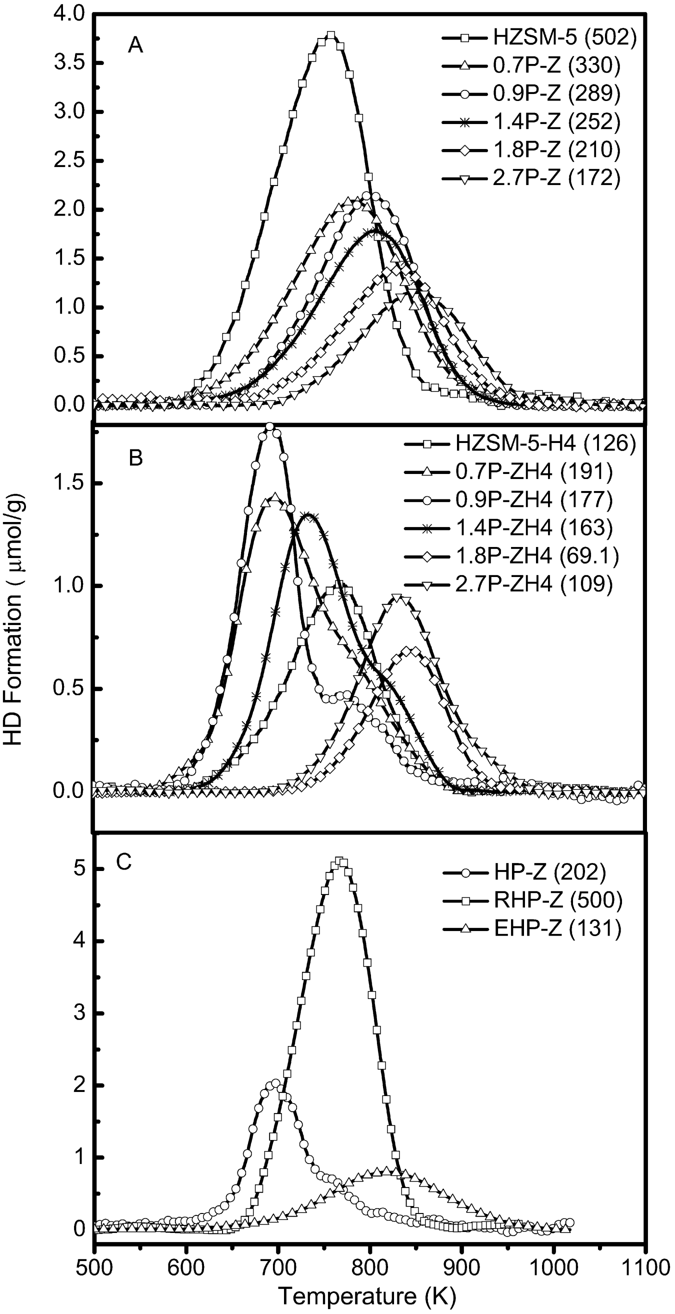

Fig. 3. D_2/OH exchange profiles of (A) P/HZSM-5 untreated by steam at 1073 K; (B) P/HZSM-5 treated by steam at 1073 K; (C) HP-Z, RHP-Z, and EHP-Z. Figures in parenthesis represent the quantities of hydroxyls measured by the D_2/OH exchange.

only ~25% (126 μmol g^{-1}) remaining from the fresh sample amount of 502 μmol g^{-1}. The exchange peak temperature remained the same as the original one, however. With the increasing phosphorous content, the D_2/OH exchange profiles exhibited complicated variations. 0.7P-ZH4 and 0.9P-ZH4 retained more OH groups than HZSM-5 after steam treatment, with the exchange peak temperature changed to 693 from 760 K. Besides the exchange peak at 693 K, a shoulder peak at ~770 K also appeared, similar to that of HZSM-5 steam-treated at the same temperature. It seems that two kinds of OH groups existed in the 0.7P-ZH4 and 0.9P-ZH4, residual zeolitic OH groups and OH groups generated during steam treatment at 1073 K, which were definitely related to the phosphorous modification (Fig. 3B). The new OH groups generated during the hydrothermal process were hydrothermally stable and responsible for the increased density of acid sites of P/HZSM-5 after hydrothermal treatment.

The new acid sites also should be formed in the other phosphorous-modified samples (e.g., 1.8P-ZH4 and 2.7P-ZH4) during hydrothermal treatment at 1073 K. However, the D_2/OH exchange profiles of the two samples were very different from those for 0.7P-ZH4 and 0.9P-ZH4. Only one resolved exchange peak appeared at 845 K (69.1 μmol g^{-1}) and 835 K (109 μmol g^{-1}) for 1.8P-ZH4 and 2.7P-ZH4, respectively. A reasonable explanation for this finding is that the overdoped phosphate condensed with the newly generated OH groups as well as with the residual zeolitic OH groups, resulting in a further decrease in the number of OH groups. Corma et al. [13] recently reported that the optimal ratio of P/Al was ca. 0.5–0.7 for the enhancement of hydrothermal stability and cracking activity of HZSM-5; the information provided by the D_2/OH exchange of this investigation seems to be in agreement with their conclusion. The two steamed samples, 0.7P-Z (P/Al ~ 0.5) and 0.9P-Z (P/Al ~ 0.64), displayed the hydroxyls with D_2/OH exchange at 693 K, and the D_2/OH exchanges were gradually postponed from 1.4P-ZH4, 1.8P-ZH4 to 2.7P-ZH4 with a reduced amount of OH groups. The 1.4P-ZH4 (with equal numbers of P and Al), showed one peak of D_2/OH exchange at 734 K and a shoulder peak at 820 K. The peak at 734 K should be related to the new OH groups, and the peak at 820 K is related to the OH groups from condensed phosphates.

To examine the nature of the newly formed hydroxyls during steam treatment of P/HZSM-5, HP-Z was designed and prepared by a hydrothermal solution method. Consistently, a similar D_2/OH exchange peak at 693 K (Fig. 3C, HP-Z) was observed, together with a shoulder peak at 760 K arose from the original hydroxyls of dealuminated HZSM-5. It should be noted that steam treatment at 1073 K was not performed for this sample. The number of OH groups, characterized by the 693 K peak of D_2/OH exchange, was almost equal to the P content in HP-Z measured by chemical analysis. But for RHP-Z, almost no P species was detected by chemical analysis, reflecting the fact that phosphate cannot condense with OH groups of HZSM-5 under the hydrothermal conditions in aqueous solution. The D_2/OH exchange was observed at 760 K (Fig. 3C), the same as for the fresh HZSM-5. For the EHP-Z sample, excessive phosphorus interacting with the new hydroxyl, the broad HD evolution peak centered at 813 K was observed again (Fig. 3C), similar to the 1.8P-ZH4 and 2.7P-ZH4 samples. Thus, the P species must relate to the silanol nests left by dealumination and the nonframework aluminum, and will affect the properties of the OH groups.

The results suggest that the hydrothermal postsynthesis in solution (HP-Z) can simulate the steam treatment at 1073 K. Furthermore, silanol nests left by dealumination seem to be necessary to form the new sites. ^{31}P NMR and D_2/OH exchange results lead to the conclusion that for the new acid sites, the

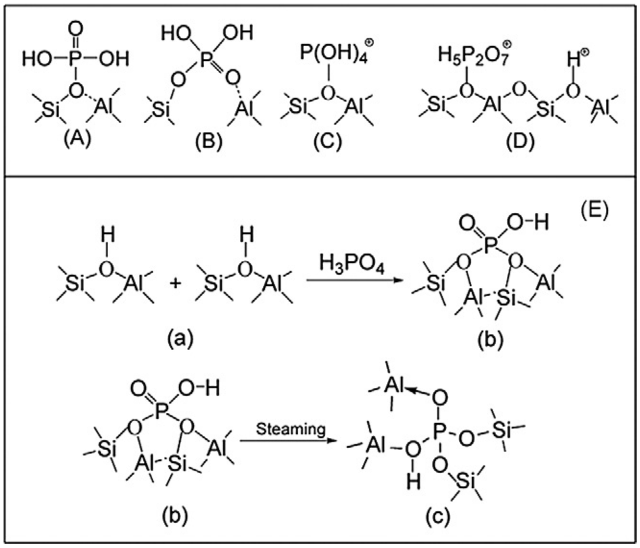

Fig. 4. Models proposed for the interaction of phosphorus with the Brönsted acid sites of HZSM-5 prepared by impregnation with phosphorus modifiers and calcinations. (A) proposed by Kaeding et al. [14] and Vedrine et al. [15]; (B) proposed by Lercher et al. [16], (C) and (D) proposed by Corma et al. [13]; (E) proposed in this work.

interaction between phosphorus and the vacancies left by dealumination and nonframework aluminum are important.

At present, it remains difficult to describe the exact structure of the new acids formed in P/HZSM-5 during steam treatment. As early as 1986, Lercher et al. [16] proposed a model to describe the interaction between the bridged hydroxyls of ZSM-5 and orthophosphoric acid. Corma et al. recently summarized the models appearing in the literature describing the interaction between HZSM-5 and phosphorous species for elucidation of the status of phosphorus species and hydroxyl groups [13–16, 19]. One widely stated view is that the framework aluminum, or a part of the framework aluminum, is stabilized via the interaction with phosphorus species; this has been convincingly supported by ^{27}Al-NMR measurements. However, these models cannot explain the changes in the number of OH groups in a series of P/HZSM-5 catalysts. Apparently, a convincing model to elucidate the structure of the modified acid sites has not yet been proposed.

To summarize the current results, Fig. 4 shows the schematic mechanisms for the phosphorus interacting with HZSM-5 (Fig. 4E), along with other previously proposed models (Figs. 4A, 4B, 4C, and 4D). It seems that these latter four models cannot account for the change in the number of OH groups. According to the model shown in Fig. 4E, two zeolitic hydroxyls condensed with one phosphate molecule before the steam treatment but calcined in dry air, leading to a decrease in the number of OH groups on P modification [Fig. 4E(b)], in agreement with the results of Corma et al. [13]. During the steam treatment (dealumination), some zeolitic OH groups, $(SiO)_4Al–H$, were substituted by phosphorous hydroxyls (P–OH), stabilized by nonframework Al, which are hydrothermally stable [Fig. 4E(c)].

Through careful two-dimensional NMR measurements of ^{27}Al, ^{29}Si, and ^{31}P, Zhuang et al. [11] proposed that the P occupied framework silicon positions of ZSM-5 to form $(SiO)_xAl(PO)_{4-x}$species after steam treatment at high temperature. The results appear to be convincing to elucidate the entrance of P into the framework. But the structure of $(SiO)_xAl(PO)_{4-x}$seems questionable, for the P–Al pair produces no hydroxyl groups due to neutralization of charges. More recently, Blasco et al. [13] proposed a new model concerning the interaction between orthophosphoric acid and bridged hydroxyls before steam treatment. They proposed that the phosphorous stabilized framework aluminum pairs (Figs. 4C and 4D); our current results support this proposal. However, the situation changed due to steam treatment at high temperatures; a new kind of OH group formed with the D_2/OH exchange peak at ∼693 K. We believe that the phosphorous entered the framework by occupying the vacancy left by dealumination during steam treatment. The entering framework of P stabilized by nonframework Al resulted in a new kind of acid site that is hydrothermally stable.

The local phosphorus structure in HZSM-5 would be deduced from the aforementioned results. It is rational to describe the structure of P species as shown in Fig. 4E. The chemical shift at −23 ppm may be assigned to the new P species formed during the steam treatment at 1073 K. Recently, Afeworki et al. [41] reported a new microporous material, EMM-3, which is a kind of SAPO material. The P species with NMR chemical shift at −23 ppm was found for their SAPO EMM-3 mesoporous material. Through a combination of our D_2/OH exchange and ^{31}P MAS NMR measurements, we can conclude that the newly formed acids in P/HZSM-5 steamed at 1073 K are similar to some kinds of SAPO in local structure.

Table 2
Cell parameters of modified zeolite determined by XRD measurements

Samples	a (Å)	b (Å)	c (Å)	V (Å^3)	R_V[a]
HZSM-5	20.15	19.79	13.22	5270.8	100
HZSM-5-H4	20.11	19.75	13.06	5185.2	98.4
0.9P-Z	20.08	19.80	13.21	5253.4	99.7
0.9P-ZH4	20.09	19.77	13.23	5254.5	99.7
1.8P-Z	20.12	19.79	13.21	5260.9	99.8
1.8P-ZH4	20.12	19.78	13.20	5254.8	99.7
2.7P-Z	20.11	19.79	13.23	5266.7	99.9
2.7P-ZH4	20.10	19.77	13.20	5244.5	99.5
HP-Z	20.12	19.77	13.08	5200.9	98.7

[a] Relative crystal cell volumes.

3.3. Crystal lattice parameters

Crystal lattice parameters determined by XRD for the samples are listed in Table 2. The undoped HZSM-5 showed a significant decrease in cell volume after steam treatment. The shrinkage in cell volume was prohibited by P doping. Apparently, dealumination was particularly prevented by the P doping. However, D_2/OH measurements revealed that only ∼25% of hydroxyls were reserved after steam treatment, regardless of whether or not the P was doped, meaning that the most aluminum could not produce hydroxyl groups. Our point is that the phosphorus can enter the framework of HZSM-5 during steam treatment at 1073 K to maintain crystal lattice parameters and to stabilize the residual framework aluminum, together with some extra-framework Al.

3.4. NH_3-TPD

The results of NH_3-TPD of the catalysts are presented in Fig. 5. Generally, two desorption maxima can be seen from the TPD curves, which define weak and strong acid sites, respectively. The peak at higher temperature is due to desorption of ammonia chemisorbed at strong acid sites (zeolitic OH sites), whereas that at lower temperature is assigned to weak acid sites (Fig. 5A). The two peaks overlapped significantly for all of the samples, especially for the P-doped HZSM-5. With increasing phosphorus loading, the densities of strong acid sites decreased, while the densities of weak acid sites increased. Fig. 5B shows the ammonia desorbed only from the strong acid sites by flushing the sample at 573 K to remove the weakly bonded ammonia before NH_3-TPD measurement. The acidic strength and the acid site density decreased gradually with increasing phosphorus content, reflecting replacement of the strong bridged hydroxyls by a new type of acid site with reduced acid strength, according to the model proposed in Fig. 4E.

Fig. 5C shows NH_3-TPD curves of the steam-treated and postsynthesis samples; only the results of HZSM-5-H4, 0.9P-ZH4, and HP-Z are given as representative. Adsorption of NH_3 was performed at 573 K for 0.5 h. The treatment in steam at 1073 K for 4 h sharply reduced the amount of adsorbed ammonia for all of the catalysts regardless of whether or not the P was doped. But the phosphorus-modified HZSM-5 (Fig. 5C, 0.9P-ZH4) reserved more acid sites compared with HZSM-5-H4. Seemingly, the dealumination from framework by steaming was inhibited to some extent by phosphorus modification. Unfortunately, the number of acid sites (especially of the strong Brönsted acids), was difficult to detect accurately by NH_3-TPD at a low density level. As shown by the NH_3-TPD profiles, the 0.9P-ZH4 and H-PZ samples were of weaker acidity than HZSM-5 but stronger than HZSM-5-H4, in accord with the results of D_2/OH exchange. These results show the similarity of HP-Z and 0.9P-ZH4 in zeolitic acid.

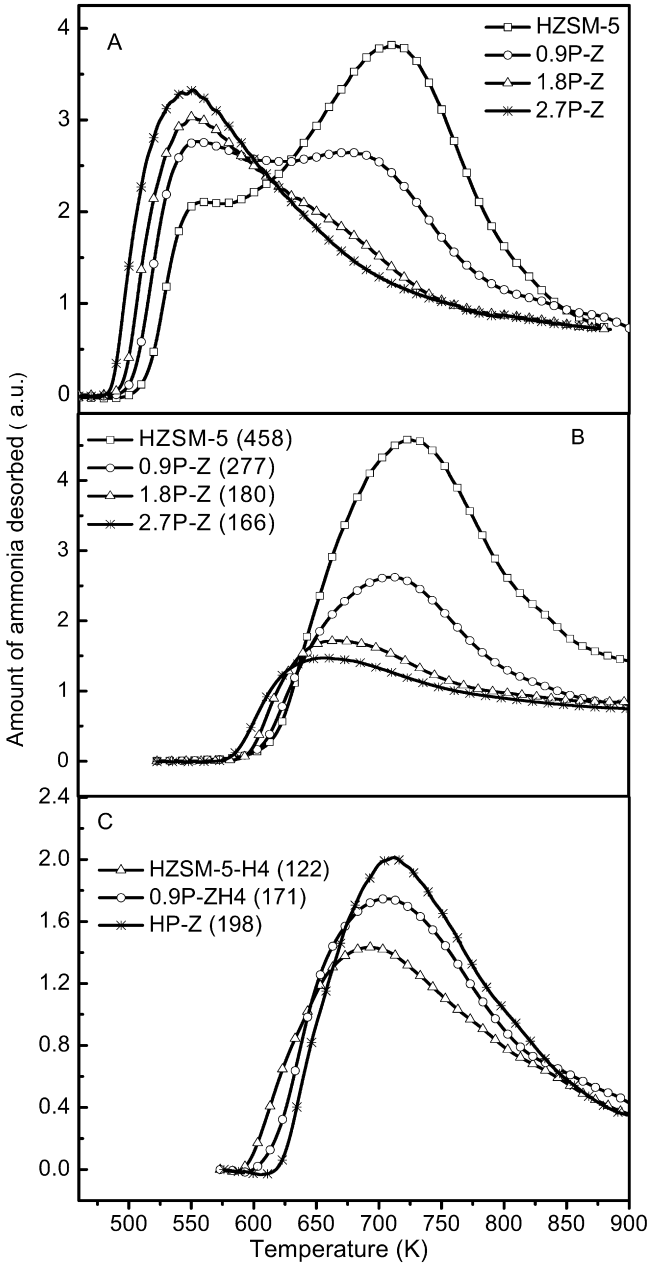

Fig. 5. NH_3-TPD profiles of (A) fresh and phosphorus-modified HZSM-5; (B) fresh and phosphorus-modified HZSM-5 at high temperature region; (C) HZSM-5-H4, 0.9P-ZH4, and HP-Z.

3.5. Cracking of C_4 olefins

The effect of phosphorus modification on the catalytic performance of P/HZSM-5 for C_4 olefin cracking was evaluated; the results are listed in Table 3. Apparently, the performance of

Table 3
The catalytic performance of P/HZSM-5 for butene cracking before and after steam treatment

Samples	$C_4^=$ conversion (%)[a]		$C_3^=$ yield (%)[a]		$C_2^=$ yield (%)[a]		C_5^+ yield (%)[a]	
	Untreated[b]	Treated[c]	Untreated[b]	Treated[c]	Untreated[b]	Treated[c]	Untreated[b]	Treated[c]
HZSM-5	94.4	59.7	14.4	35.2	13.9	6.7	37.5	16.7
0.9P-Z	85.7	82.6	28.2	33.1	19.9	21.9	21.0	13.6
1.8P-Z	66.1	75.5	38.4	43.1	9.61	12.8	15.4	9.2
2.7P-Z	10.4	53.1	5.03	31.2	0.35	5.0	5.7	14.6

[a] All the data were obtained at 6 h on stream.

[b] The catalysts were prepared by impregnation and calcined without steam treatment.

[c] The catalysts were treated in 100% steam at 1073 K for 4 h before catalytic test.

HZSM-5 for C_4 olefin cracking decreased due to the 4-h steam treatment at 1073 K before the cracking test. The C_4 olefin conversion over the HZSM-5 decreased significantly, whereas the selectivity to $C_{2–3}$ olefins increased. Referring to the results of D_2/OH exchange and NH_3-TPD, the decrease in C_4 olefin conversion can be ascribed mainly to the decreased acid strength and density due to the steam treatment. According to the mechanism of olefin cracking reported in Refs. [42–45] and our work (not shown), the butene first dimerized to C_8 hydrocarbons and later cracked to smaller molecules. Along with propene and ethene, methane, ethane, butane and hydrocarbons with more than 4 carbon atoms (namely C_5^+) also were detected. The yields of C_5^+ (i.e., the sums of all C_5^+ hydrocarbons) are also listed in Table 3.

P modification significantly improved the stability of the catalytic performance of HZSM-5 against the steam treatment and also enhanced the yield of $C_{2–3}$ olefins. Before the steam treatment, however, P doping caused a sharp decrease in C_4 conversion with increasing P content. This should be due to the reduced density of the acid sites and decreased surface area and pore volume, as shown in Table 4. The steam treatment at 1073 K altered the situation significantly, as shown in Table 3. The selectivity to $C_{2–3}$ olefins was greatly enhanced for 0.9P-ZH4, even though the conversion of C_4 olefin was slightly depressed. But for the 1.8P-ZH4 and 2.7P-ZH4, with the amount of P surpassing the amount of aluminum, both the conversion of C_4 olefin and the selectivity to $C_{2–3}$ olefins were significantly promoted by the steam treatment at 1073 K. This enhancement is correlated to the removal of some overdoped P, or the incorporation of some P into the framework of zeolite, as well as to the refurbishing of the surface area and pore volume during the steam treatment, as shown in Table 4. This also implies that the overdoped phosphorous species were not so stable in HZSM-5 during the steam treatment and they interacted weakly with the zeolite framework by condensation with bonded phosphate, in agreement with the ^{31}P-NMR measurements. The polyphosphates were unstable in steam, and some were lost during steam treatment, as shown in Table 1. Along with the lost phosphorus, the increased surface area and pore volume also may be ascribed to incorporation of P into the lattice and formation of better-organized framework structures as cell parameters, as shown in Table 2.

Table 4
The effect of phosphorus modification on surface area and pore volume of HZSM-5

	Surface area ($m^2\,g^{-1}$)	Pore volume ($cm^3\,g^{-1}$)
HZSM-5	386	0.22
0.9P-Z	299	0.16
1.8P-Z	248	0.14
2.7P-Z	213	0.12
0.9P-ZH4	308	0.17
1.8P-ZH4	306	0.16
2.7P-ZH4	284	0.14

To investigate the effect of P modification on the stability of catalytic performance for C_4 olefin cracking, the 0.9P-Z sample was treated under severe conditions (i.e., in 100% steam at 1073 K) for a prolonged time. Table 5 gives the catalytic results, along with the properties of the HZSM-5 treated under the same conditions for comparison. For HZSM-5, the 1-butene conversion and propene and ethene yields decreased sharply with prolonged steaming time, but for 0.9P-Z, high and stable yields of propene and ethene were observed. The slightly decreased olefin conversion was compensated for by the reduced C_5^+ yields. Improved selectivity to propene was observed with prolonged time of steam treatment. This finding is very important for catalyst design and industry applications. As mentioned earlier, the acidity of HP-Z was similar to that of 0.9P-ZH4. Consistently, the catalytic properties of HP-Z for the reaction under the same conditions were also similar to those of 0.9P-ZH4, as shown in Table 5. This is in agreement with the foregoing discussion on the results of D_2/OH exchange and ^{27}Al and ^{31}P NMR measurements. The varying catalytic properties of the phosphorus-modified HZSM-5 with reaction time on stream are shown in Fig. 6. The 0.9P-ZH4 shows very good, stable properties for butene cracking.

4. Conclusion

New kinds of acid sites created in phosphorus-modified HZSM-5 through treatment in 100% steam at 1073 K show much better hydrothermal stability and significantly modified catalytic performance for C_4 olefin cracking. Our investigation using D_2/OH exchange and solid-state ^{31}P and ^{27}Al NMR measurements show that the new acid sites seem to be related to the

Table 5
Catalytic performance of HZSM-5 and phosphorus modified HZSM-5 before and after steam treatment for varied time

	T_p[a] (K)	[OH] (μmol g^{-1})	$C_4^=$ conversion (%)	$C_3^=$ yield (%)	$C_2^=$ yield (%)	$C_3^= + C_2^=$ yield (%)	C_5^+ yield (%)
HZSM-5	760	502	94.4	14.4	13.9	28.3	37.5
HZSM-5-H4	765	126	59.7	35.2	6.7	41.9	16.7
HZSM-5-H12	783	150	44.0	23.5	3.1	26.6	9.7
HZSM-5-H48	786	130	25.9	13.2	1.2	14.4	8.6
0.9P-Z	813	289	85.7	28.2	20.0	48.2	21.0
0.9P-ZH4	693	177	82.6	33.1	21.9	55.0	13.6
0.9P-ZH12	693	109	76.4	40.1	17.4	57.5	5.63
0.9P-ZH48	693	93	73.1	42.5	14.2	56.7	4.36
HP-Z	693	202	79.6	37.6	21.5	59.1	12.1

[a] T_p means the HD evolution peak temperature for D_2/OH exchange. All the reaction data were collected at 6 h on stream at 803 K with olefin liquid hour space velocity of 10 h^{-1}.

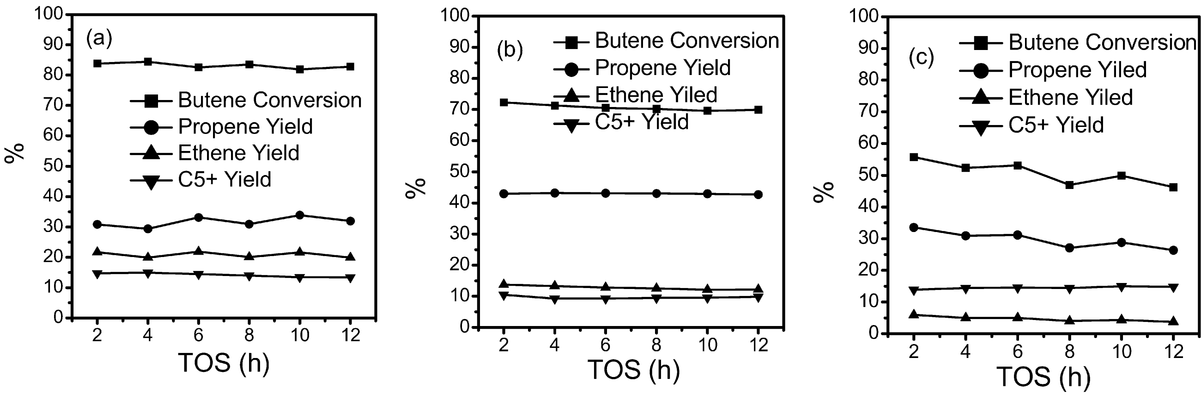

Fig. 6. Variation of catalytic performance with time on stream of 1-butene cracking. (a) 0.9P-ZH4; (b) 1.8P-ZH4; (c) 2.7P-ZH4.

phosphorus entering into the zeolitic position left by dealumination and stabilized by some extra-lattice aluminum. The entry of phosphorus into the zeolitic framework protects the residual framework aluminum against further dealumination. The integrated effect causes the hydrothermally stable acid sites in P-modified HZSM-5 and enhances the catalytic performance for C_4 olefin cracking after steam treatment at high temperature. The mechanism reported herein should be very important in zeolite applications for hydrocarbon reactions.

Acknowledgments

This project was supported by the Ministry of Science and Technology of China (grant 2003CB615804) and the Natural Science Foundation of China (grants 20403008 and 20673054). The authors thank Professor Roel Prins for helpful discussions, Mr. Yao Yu for help with the NMR measurements, Drs. Jiawei Teng and Yangdong Wang for help with the catalytic tests, and Professor Lin Dong.

References

[1] A. de Lucas, P. Canizares, A. Duran, A. Carrero, Appl. Catal. A 154 (1997) 221.
[2] S. Liu, R. Ohnishi, M. Ichikawa, J. Catal. 220 (2003) 57.
[3] Y. Lu, M. He, X. Shu, B. Zong, Appl. Catal. A 255 (2003) 345.
[4] B. Wang, Q. Gao, J. Gao, D. Ji, X. Wang, J. Suo, Appl. Catal. A 274 (2004) 167.
[5] X. Zhu, S. Liu, Y. Song, L. Xu, J. Catal. 288 (2005) 124.
[6] X. Zhu, S. Liu, Y. Song, S. Xie, L. Xu, Appl. Catal. A 290 (2005) 191.
[7] X. Zhu, S. Liu, Y. Song, L. Xu, Catal. Lett. 103 (2005) 201.
[8] G. Zhao, J. Teng, Y. Zhang, Z. Xie, Y. Yue, Q. Chen, Y. Tang, Appl. Catal. A 299 (2006) 167.
[9] G. Lischke, R. Eckelt, H.-G. Jerschkewitz, B. Parlitz, E. Schreier, W. Storek, B. Zibrowius, G. Ohlmann, J. Catal. 132 (1991) 229.
[10] G. Ohlmann, H.-G. Jerschkewitz, G. Lischke, R. Eckelt, B. Parlitz, E. Schreier, B. Zibrowius, E. Loeffler, Stud. Surf. Sci. Catal. 65 (1991) 1.
[11] J. Zhuang, D. Ma, G. Yang, Z. Yan, X. Liu, X. Liu, X. Han, X. Bao, P. Xie, Z. Liu, J. Catal. 228 (2004) 234.
[12] G. Yang, J. Zhuang, Y. Wang, D. Zhou, M. Yang, X. Liu, X. Han, X. Bao, J. Mol. Struct. 737 (2005) 271.
[13] T. Blasco, A. Corma, J. Martínez-Triguero, J. Catal. 237 (2006) 267.
[14] W.W. Kaeding, S.A. Butter, J. Catal. 61 (1980) 155.
[15] J.C. Vedrine, A. Auroux, P. Dejaifve, V. Ducarme, H. Hoser, S. Zhou, J. Catal. 73 (1982) 147.
[16] J.A. Lercher, G. Rumplmayr, Appl. Catal. 25 (1986) 215.
[17] A. Rahman, G. Lemay, A. Adnot, S. Kaliaguine, J. Catal. 112 (1988) 453.
[18] H. Vinek, G. Rumplmayr, J.A. Lercher, J. Catal. 115 (1989) 291.
[19] P. Tynjala, T.T. Pakkanen, Micropor. Mesopor. Mater. 20 (1998) 363.
[20] A. Jentys, G. Rumplmayr, J.A. Lercher, Appl. Catal. 53 (1989) 299.
[21] G. Seo, R. Ryoo, J. Catal. 124 (1990) 224.
[22] M. Kojima, F. Lefebvre, Y.B. Taarit, Zeolites 12 (1992) 724.
[23] I. Hannus, I. Kiricsi, P. Fejes, A. Fonseca, J.B. Nagy, W.O. Parker Jr., Z. Szendi, Zeolites 16 (1996) 142.
[24] T. Bernstein, P. Fink, V.M. Mastikhin, A.A. Shubin, J. Chem. Soc. Faraday Trans. 82 (1986) 1879.
[25] A.R. Grimmer, U. Haubenreisser, Chem. Phys. Lett. 99 (1983) 487.
[26] T.M. Duncan, D.C. Douglass, Chem. Phys. 87 (1984) 339.
[27] G. Caeiro, P. Magnoux, J.M. Lopes, F. Ramoa Ribeiro, S.M.C. Menezes, A.F. Costa, H.S. Cerqueira, Appl. Catal. A 314 (2006) 160.
[28] K. Damodaran, J.W. Wiench, S.M. Cabral de Menezes, Y.L. Lam, J. Trebosc, J.-P. Amoureux, M. Pruski, Micropor. Mesopor. Mater. 95 (2006) 296.
[29] A. Gola, B. Rebours, E. Milazzo, J. Lynch, E. Benazzi, S. Lacombe, L. Delevoye, C. Fernandez, Micropor. Mesopor. Mater. 40 (2000) 73.
[30] C.S. Blackwell, R.L. Patton, J. Phys. Chem. 88 (1984) 6135.
[31] D. Muller, E. Jahn, G. Ludwig, Chem. Phys. Lett. 109 (1984) 332.
[32] I.L. Mudrakowski, V.M. Mastikhin, V.P. Shmachkova, N.S. Kotsarenko, Chem. Phys. Lett. 120 (1985) 424.
[33] Z. Yan, D. Ma, J. Zhuang, X. Liu, X. Liu, X. Han, X. Bao, F. Chang, L. Xu, Z. Liu, J. Mol. Catal. A 194 (2003) 153.
[34] J.X. Chen, T.H. Chen, N.J. Guan, J.Z. Wang, Catal. Today 93–95 (2004) 627.
[35] S.M.C. Menezes, V.L. Camorim, Y.L. Lam, R.A.S. San Gil, A. Bailly, J.P. Amoureux, Appl. Catal. A 207 (2001) 367.
[36] T.H. Chen, B.H. Wouters, P.J. Grobet, Eur. J. Inorg. Chem. 2 (2000) 281.
[37] J.A. Biscardi, G.D. Meitzner, E. Iglesia, J. Catal. 179 (1998) 192.
[38] W.P. Ding, G.D. Meitzner, D.O. Marler, E. Iglesia, J. Phys. Chem. B 105 (2001) 3928.
[39] W.P. Ding, S.Z. Li, G.D. Meitzner, E. Iglesia, J. Phys. Chem. B 105 (2001) 506.
[40] W.P. Ding, G.D. Meitzner, E. Iglesia, J. Catal. 206 (2002) 14.
[41] M. Afeworki, G.J. Kennedy, D.L. Dorset, K.G. Strohmaier, Chem. Mater. 18 (2006) 1705.
[42] M. Guisnet, P. Andy, N.S. Gnep, E. Benazzi, C. Travers, J. Catal. 158 (1996) 551.
[43] P. Mériaudeau, R. Bacaud, L. Ngoc Hung, A.T. Vu, J. Mol. Catal. A 110 (1996) L177.
[44] C. Pazè, B. Sazak, A. Zecchina, J. Dwyer, J. Phys. Chem. B 103 (1999) 9978.
[45] O. Bortnovsky, P. Sazama, B. Wichterlova, Appl. Catal. A 287 (2005) 203.